Chapter 2

Main machine layout and performance

2.1 Performance goals

The aim of the LHC is to reveal the physics beyond the Standard Model with centre of mass collision energies of up to 14 TeV. The number of events per second generated in the LHC collisions is given by:

$$N_{\text{event}} = L\sigma_{\text{event}} \tag{2.1}$$

where σ_{event} is the cross section for the event under study and L the machine luminosity. The machine luminosity depends only on the beam parameters and can be written for a Gaussian beam distribution as:

$$L = \frac{N_b^2 n_b f_{\text{rev}} \gamma_r}{4\pi\varepsilon_n \beta*} F \tag{2.2}$$

where N_b is the number of particles per bunch, n_b the number of bunches per beam, f_{rev} the revolution frequency, γ_r the relativistic gamma factor, ε_n the normalized transverse beam emittance, $\beta*$ the beta function at the collision point, and F the geometric luminosity reduction factor due to the crossing angle at the interaction point (IP):

$$F = \left(1 + \left(\frac{\theta_c \sigma_z}{2\sigma*}\right)^2\right)^{-1/2} \tag{2.3}$$

θ_c is the full crossing angle at the IP, σ_z the RMS bunch length, and $\sigma*$ the transverse RMS beam size at the IP. The above expression assumes round beams, with $\sigma_z \ll \beta$, and with equal beam parameters for both beams. The exploration of rare events in the LHC collisions therefore requires both high beam energies and high beam intensities.

The LHC has two high luminosity experiments, ATLAS [14] and CMS [15], both aiming at a peak luminosity of $L = 10^{34}\text{cm}^2\text{s}^1$ for proton operation. There are also two low luminosity experiments: LHCB [16] for B-physics, aiming at a peak luminosity of $L = 10^{32}\text{cm}^2\text{s}^1$, and TOTEM [17] for the detection of protons from elastic scattering at small angles, aiming at a peak luminosity of $L = 2 \times 10^{29}\text{cm}^2\text{s}^1$ with 156 bunches. In addition to the proton beams, the LHC will also be operated with ion beams. The LHC has one dedicated ion experiment, ALICE [18], aiming at a peak luminosity of $L = 10^{27}\text{cm}^2\text{s}^1$ for nominal lead-lead ion operation.

The high beam intensity required for a luminosity of $L = 10^{34}\text{cm}^2\text{s}^1$ excludes the use of anti-proton beams, and hence excludes the particle-anti-particle collider configuration of a common vacuum and magnet system for both circulating beams, as used for example in the Tevatron. To collide two counter-rotating proton beams requires opposite magnetic dipole fields in both rings. The LHC is therefore designed as a proton-proton collider with separate magnet fields and vacuum chambers in the main arcs and with common sections only at the insertion regions where the experimental detectors are located. The two beams share an approximately 130 m long common beam pipe along the IRs. The exact length is 126 m in IR2 and IR8, which feature superconducting separation dipole magnets next to the triplet assemblies, and 140 m in IR1 and IR5, which feature normal conducting magnets and therefore longer separation dipole magnets next to the triplet assemblies. Together with the large number of bunches (2'808 for each proton beam), and a nominal bunch spacing of 25 ns, the long common beam pipe implies 34 parasitic collision points at each experimental insertion region. For four experimental IRs, this implies a total of 136 unwanted collision points. Dedicated crossing angle orbit bumps separate the two LHC beams left and right from the IP in order to avoid collisions at these parasitic collision points.

There is not enough room for two separate rings of magnets in the LEP/LHC tunnel and, for this reason, the LHC uses twin bore magnets that consist of two sets of coils and beam channels within the same mechanical structure and cryostat. The peak beam energy depends on the integrated dipole field around the storage ring, which implies a peak dipole field of 8.33 T for the 7 TeV in the LHC machine and the use of superconducting magnet technology.

2.2 Performance limitations

2.2.1 Beam-beam limit

The maximum particle density per bunch is limited by the nonlinear beam-beam interaction that each particle experiences when the bunches of both beams collide with each other. The beam-beam interaction is measured by the linear tune shift given by:

$$\xi = \frac{N_b\, r_p}{4\pi\varepsilon_n} \tag{2.4}$$

in which r_p is the classical proton radius $r_p = e^2/(4\pi\varepsilon_0 m_p c^2)$. Experience with existing hadron colliders indicates that the total linear tune shift summed over all IPs should not exceed 0.015. With three proton experiments requiring head-on collisions, this implies that the linear beam-beam tune shift for each IP should satisfy $\xi < 0.005$.

2.2.2 Mechanical aperture

The geometrical aperture of the LHC arcs is given by the beam screen dimensions. The beam screen has a height of approximately 2×17.3 mm and a total width of 2×22 mm. Setting the minimum aperture of 10 σ in terms of the RMS beam size, and allowing for tolerances for the linear machine imperfections and the magnet alignment and geometry, implies a peak nominal beam size of 1.2 mm. The minimum mechanical aperture of 10 σgs prescribed by the LHC beam cleaning system. When combined with a peak β-function of 180 m in the LHC arcs, this implies a maximum

2008 JINST 3 S08001

acceptable transverse beam emittance of $\varepsilon_n = 3.75\ \mu$m. The limit on the linear beam-beam tune shift and the mechanical aperture of the LHC therefore limit the maximum bunch intensity to $N_b = 1.15 \times 10^{11}$.

Furthermore, the mechanical aperture of the triplet magnets limits the minimum attainable β^* value at the IPs and the maximum attainable crossing angle orbit bump in the experimental interaction regions. Both these parameters limit the peak luminosity in the LHC machine.

2.2.3 Maximum dipole field and magnet quench limits

The maximum beam energy that can be reached in the LHC is limited by the peak dipole field in the storage ring. The nominal field is 8.33 T, corresponding to an energy of 7 TeV. However, the actual field attainable in the storage ring depends on the heat load and temperature margins inside the cryo-magnets and therefore on the beam losses during operation. A high dipole field therefore requires efficient operation with minimum beam losses.

2.2.4 Energy stored in the circulating beams and in the magnetic fields

A total beam current of 0.584 A corresponds to a stored energy of approximately 362 MJ. In addition to the energy stored in the circulating beams, the LHC magnet system has a stored electromagnetic energy of approximately 600 MJ, yielding a total stored energy of more than 1 GJ. This stored energy must be absorbed safely at the end of each run or in the case of a malfunction or an emergency. The beam dumping system and the magnet system therefore provide additional limits for the maximum attainable beam energies and intensities.

2.2.5 Heat load

Although synchrotron radiation in hadron storage rings is small compared to that generated in electron rings, it can still impose practical limits on the maximum attainable beam intensities, if the radiation has to be absorbed by the cryogenic system. In addition to the synchrotron-radiation heat load, the LHC cryogenic system must absorb the heat deposition from luminosity-induced losses, impedance-induced losses (resistive wall effect) and electron-cloud bombardment.

2.2.6 Field quality and dynamic aperture

Field quality errors compromise the particle stability in the storage ring, and hence loss-free operation requires a high field quality. A characterizing feature of superconducting magnets is the decay of persistent currents and their 'snap back' at the beginning of the ramp. Achieving small beam losses therefore requires a tight control of the magnetic field errors during magnet production and during machine operation. Assuming fixed limits for the beam losses (set by the quench levels of the superconducting magnets), the accuracy of the field quality correction during operation and its limitation on machine performance can be estimated.

2008 JINST 3 S08001

2.2.7 Collective beam instabilities

The interaction of the charged particles in each beam with each other via electromagnetic fields and the conducting boundaries of the vacuum system can result in collective beam instabilities. Generally speaking, the collective effects are a function of the vacuum system geometry and its surface properties. They are usually proportional to the beam currents and can therefore limit the maximum attainable beam intensities.

2.2.8 Luminosity lifetime

The luminosity in the LHC is not constant over a physics run, but decays due to the degradation of intensities and emittances of the circulating beams. The main cause of the luminosity decay during nominal LHC operation is the beam loss from collisions. The initial decay time of the bunch intensity, due to this effect, is:

$$\tau_{\text{nuclear}} = \frac{N_{\text{tot},0}}{L\sigma_{\text{tot}}k} \tag{2.5}$$

where $N_{\text{tot},0}$ is the initial beam intensity, L the initial luminosity, $\sigma_{\text{tot}}$the total cross section (σ_{tot} = 10^{25} cm^{-2} at 14TeV) and k the number of IPs. Assuming an initial peak luminosity of L = 10^{34} cm^{-2}s^{-1} and two high luminosity experiments, the above expression yields an initial decay time of τ = 44.85 h. Equation 2.5 results in the following decay of the beam intensity and luminosity as functions of time:

$$N_{\text{tot}}(t) = \frac{N_{\text{tot},0}}{1+t/\tau_{\text{nuclear}}} \tag{2.6}$$

$$L(t) = \frac{L_0}{(1+t/\tau_{\text{nuclear}})^2}\,. \tag{2.7}$$

The time required to reach $1/e$ of the initial luminosity is given by:

$$t_{1/e} = \left(\sqrt{e}-1\right)\tau\,, \tag{2.8}$$

yielding a luminosity decay time of $\tau_{\text{nuclear},1/e} = 29\ h$.

Other contributions to beam losses come from Toucheck scattering and from particle losses due to a slow emittance blow-up. Emittance blow-up can be caused by the scattering of particles on residual gas, the nonlinear force of the beam-beam interaction, RF noise, and IBS scattering effects.

The synchrotron radiation damping in the LHC decreases the bunch dimensions at top energy and can partially compensate the beam size blow-up due to the above effects. Following the arguments set out in the Pink Book (1991 Design Study) [19], it is assumed that the radiation damping process just cancels the beam blow up due to the beam-beam interactions and RF noise. Approximating further the decay by an exponential process, the net luminosity lifetime can be estimated as:

$$\frac{1}{\tau_L} = \frac{1}{\tau_{\text{IBS}}} + \frac{1}{\tau_{\text{rest gas}}} + \frac{1}{\tau_{\text{nuclear},1/e}} \tag{2.9}$$

Assuming an IBS time constant of 80 hour and a rest gas time constant of 100 hour with the above nuclear decay time gives a net estimate of the luminosity lifetime of,

$$\tau_L = 14.9\ h. \tag{2.10}$$

2.2.9 Average turnaround time

Filling the LHC requires 12 cycles of the SPS synchrotron, and each SPS fill requires 3 to 4 cycles of the PS synchrotron. The SPS and PS cycling time are 21.6 s and 3.6 s, respectively, yielding a total LHC filling time of approximately 4 minutes per beam. Assuming that each LHC aperture requires an additional 4 SPS cycles for the injection set up (3 pilot bunches and one nominal intensity), and that the LHC operators require at least two minutes to evaluate the measurements of each pilot bunch shot and to readjust the machine settings, the total (minimum) LHC injection time becomes 16 minutes. The minimum time required for ramping the beam energy in the LHC from 450 GeV to 7 TeV is approximately 20 minutes. After a beam abort at top energy, it takes also approximately 20 minutes to ramp the magnets down to 450 GeV. Assuming a programmed check of all main systems of say 10 minutes, the total turnaround time for the LHC is of the order of 70 minutes, which should be considered as a theoretical minimum.

After 10 years of HERA machine operation, on average, only every third proton injection leads to a successful proton fill at top energy. The average time between the end of a luminosity run and a new beam at top energy in HERA is approximately 6 hours, compared to a theoretical minimum turnaround time of approximately 1 hour, i.e., 6 times longer. Thus for a minimum turnaround time for the LHC of 1.15 hours, the practical experience at HERA implies that the average turnaround time will be 7 hours.

2.2.10 Integrated luminosity

Integrating the luminosity over one run yields,

$$L_{\text{int}} = L_0 \tau_L \left[1 - e^{-T_{\text{run}}/\tau_L}\right] \tag{2.11}$$

where T_{run} is the total length of the luminosity run. The overall collider efficiency depends on the ratio of the length of the run to the average turnaround time. Assuming the machine can be operated for 200 days per year and assuming the luminosity lifetime of 15 hours obtained earlier, the optimum run time is 12 hours or 5.5 hours, for the average turnaround times of 7 hours and 1.15 hours, respectively. This leads to a maximum total integrated luminosity per year of $80\,\text{fb}^{-1}$ to $120\,\text{fb}^{-1}$, depending on the average turnaround time of the machine.

2.3 Lattice layout

The basic layout of the LHC follows the LEP tunnel geometry: see figure 2.1. The LHC has eight arcs and eight straight sections. Each straight section is approximately 528 m long and can serve as an experimental or utility insertion. The two high luminosity experimental insertions are located at diametrically opposite straight sections: the ATLAS experiment is located at Point 1 and the CMS experiment at Point 5. Two more experimental insertions are located at Point 2 and Point 8, which also include the injection systems for Beam 1 and Beam 2, respectively. The injection kick occurs in the vertical plane with the two beams arriving at the LHC from below the LHC reference plane. The beams cross from one magnet bore to the other at four locations. The remaining four straight sections do not have beam crossings. Insertions at Points 3 and 7 each contain two collimation

2008 JINST 3 S08001

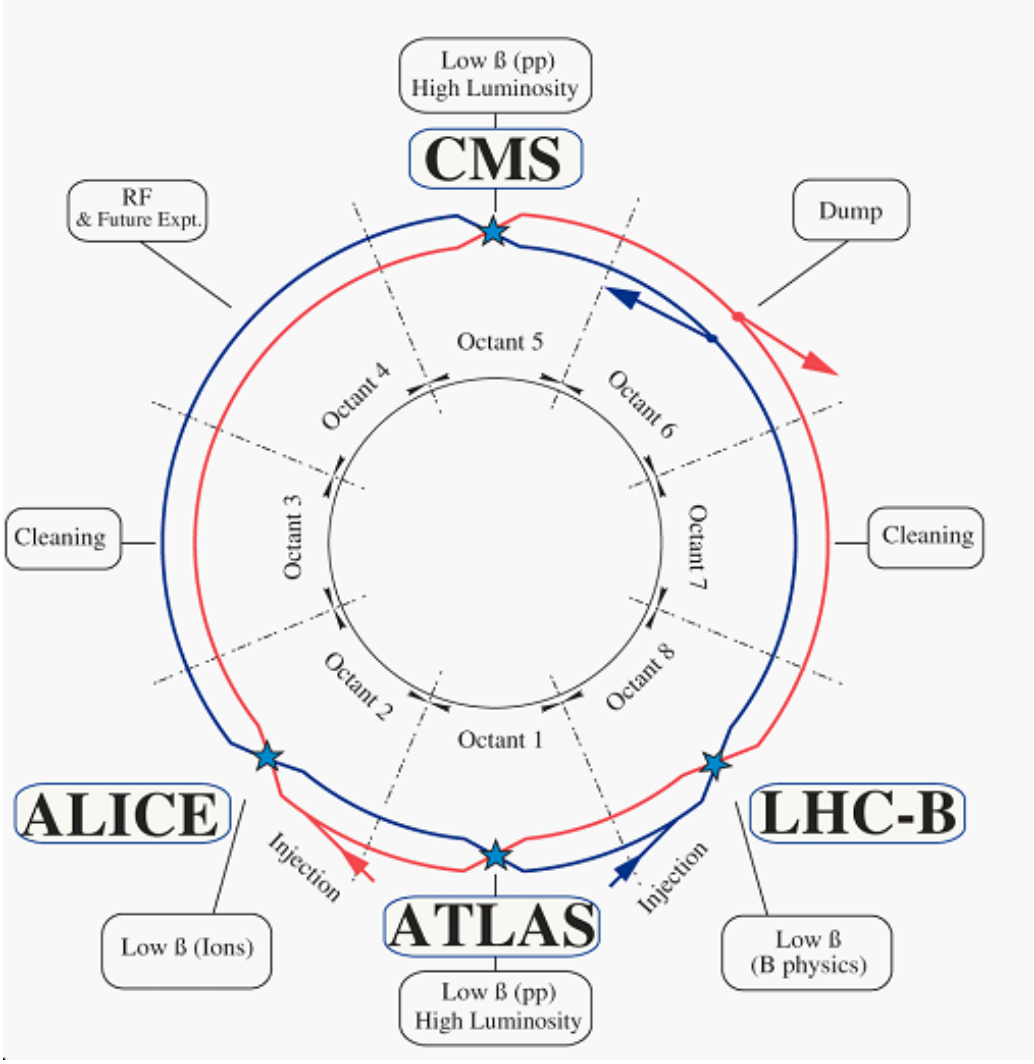

Figure 2.1: Schematic layout of the LHC (Beam 1- clockwise, Beam 2 — anticlockwise).

systems. The insertion at Point 4 contains two RF systems: one independent system for each LHC beam. The straight section at Point 6 contains the beam dump insertion, where the two beams are vertically extracted from the machine using a combination of horizontally deflecting fast-pulsed ('kicker') magnets and vertically-deflecting double steel septum magnets. Each beam features an independent abort system. The LHC lattice has evolved over several versions. A summary of the different LHC lattice versions up to version 6.4 is given in ref. [20].

The arcs of LHC lattice version 6.4 are made of 23 regular arc cells. The arc cells are 106.9 m long and are made out of two 53.45 m long half cells, each of which contains one 5.355 m long cold mass (6.63 m long cryostat), a short straight section (SSS) assembly, and three 14.3 m long dipole magnets. The LHC arc cell has been optimized for a maximum integrated dipole field along the arc with a minimum number of magnet interconnections and with the smallest possible beam envelopes. Figure 2.2 shows a schematic layout of one LHC half-cell.

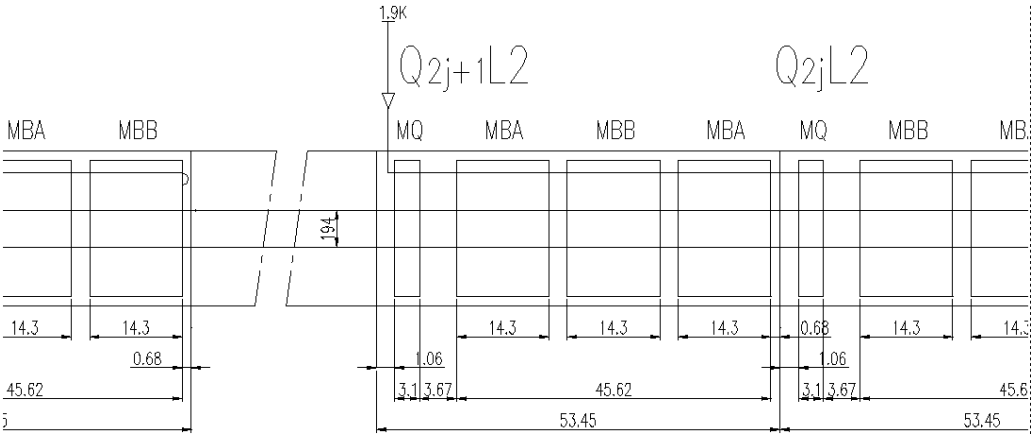

Figure 2.2: Schematic layout of an LHC half cell (distances in m).

The two apertures of Ring 1 and Ring 2 are separated by 194 mm. The two coils in the dipole magnets are powered in series, and all dipole magnets of one arc form one electrical circuit. The quadrupoles of each arc form two electrical circuits: all focusing quadrupoles in Beam 1 and Beam 2 are powered in series, and all defocusing quadrupoles in Beam 1 and Beam 2 are powered in series. The optics of Beam 1 and Beam 2 in the arc cells is therefore strictly coupled via the powering of the main magnetic elements.

A dispersion suppressor is located at the transition between an LHC arc and a straight section, yielding a total of 16 dispersion suppressor sections. The aim of the dispersion suppressors is threefold:

- Adapt the LHC reference orbit to the geometry of the LEP tunnel.
- Cancel the horizontal dispersion arising in the arc and generated by the separation / recombination dipole magnets and the crossing angle bumps.
- Facilitate matching the insertion optics to the periodic optics of the arc.

A generic design of a dispersion suppressor uses standard arc cells with missing dipole magnets. The LEP dispersion suppressor, which defined the geometry of the tunnel, was made of 3.5 cells with a 90° phase advance. With the 2.5 times longer LHC dipole and quadrupole magnets, only two LHC cells can fit in the same distance. This layout can still accurately follow the LEP tunnel geometry, but the shortened dispersion suppressor cannot fully cancel the horizontal dispersion if the dispersion suppressor cells are powered in series with the arc cells. Full cancellation of the horizontal dispersion requires individual powering of the dispersion suppressor quadrupoles. To this end, the dispersion suppressor cells are equipped with special, medium current, quadrupoles except at IR3 and IR7, which do not have enough space to house the large 6000 A power supplies required for the individual powering of the dispersion suppressor quadrupoles. Instead, the quadrupoles in these regions are powered in series with the arc quadrupoles, and each dispersion suppressor quadrupole is equipped with a trim quadrupole that requires a smaller 500 A power supply. This solution solves the space problem, but limits the flexibility in those insertions.

2008 JINST 3 S08001

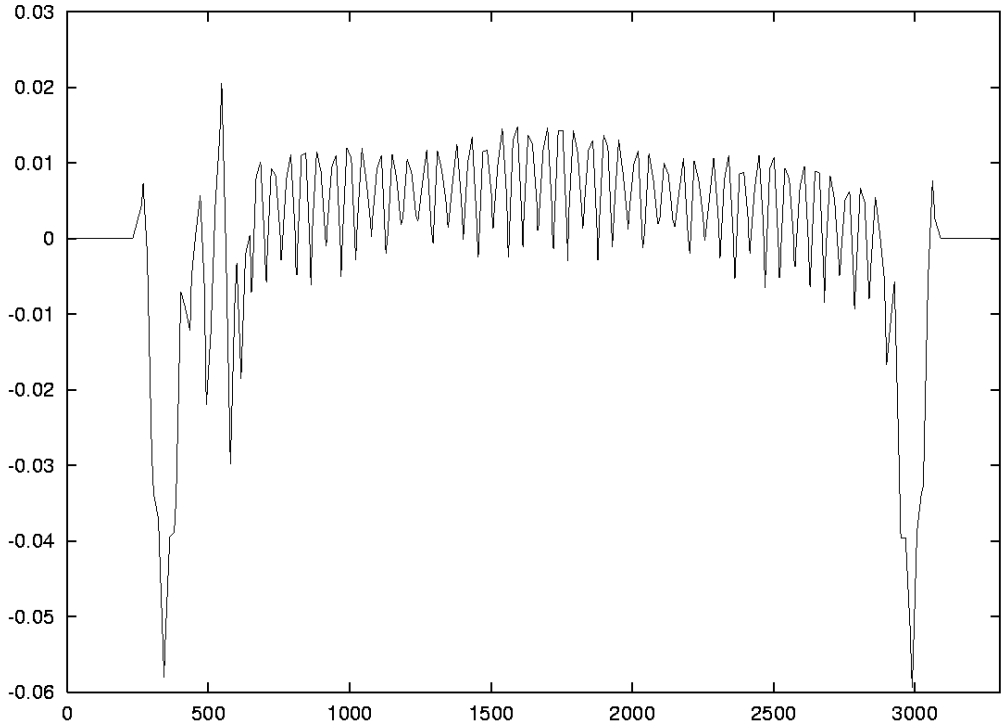

Figure 2.3: Horizontal deviation between the LHC and LEP geometries (in metres).

The straight sections in the tunnel are approximately 528 m long. A quadrupole spacing equivalent to the spacing in the arc cells allows approximately ten insertion region quadrupole magnets. The exact number and arrangement of these insertion quadrupoles depends on the requirements specific to each insertion. Assuming a midpoint symmetry for the insertion optics, this provides 5 independent parameters for matching 6 optical constraints (β_x, β_y, α_x, α_y, μ_x and μ_y) at the transition points to the dispersion suppressors, assuming that the dispersion functions can be matched via the dispersion suppressor. In order to provide the missing flexibility for matching, the dispersion suppressors are used as optical buffers between the arc and the insertion. In fact, the dispersion suppressors have to be extended into the neighbouring arcs using the arc trim quadrupole of the first arc cell to add four more free parameters for the final matching. The drawback of this scheme is that it does not provide a strictly separate functionality between the dispersion suppressor and the insertion region.

The LHC arcs are mainly positioned radially to the exterior of the theoretical position of the LEP machine by up to 4 cm, with the maximum excursions occurring near the arc transition to the dispersion suppressor. However, to keep total LHC circumference equal to the LEP circumference, the positive offset of the LHC machine in the arcs is compensated by a larger excursion in the opposite direction inside the dispersion suppressors. See figure 2.3. The LHC is divided into 8 independent sectors (the arcs between two consecutive straight sections).

2.4 Corrector circuits

The corrector magnets located in the arcs of the LHC can be split into two distinct categories:

- The lattice corrector magnets placed on both sides of the main quadrupoles in the SSS cryostats.
- The spool-piece correctors which are thin nonlinear windings attached directly to the extremities of the main dipoles.

In contrast to the main dipole circuits and the two main quadrupole families, the arc corrector magnets can be adjusted independently for the two beams. The different types and main functionalities of the lattice corrector magnets are summarized below.

2.4.1 Arc orbit corrector magnets MCB

Horizontal and vertical orbit corrector magnets, MCBH and MCBV, are installed at each focusing (QF) and defocusing (QD) quadrupole respectively, making a total of 23 or 24 orbit correctors per ring, per arc and per transverse plane, depending on the polarity of the quadrupole at mid-arc. They are designed to achieve a maximum kick of 80.8 μrad at 7 TeV for a nominal current of 55 A.

2.4.2 Chromaticity or lattice sextupoles, MS

Chromaticity sextupoles, MS, are installed at each focusing and defocusing quadrupole of the lattice. The chromaticity sextupoles are split into four families in each sector of each ring. Two families, SF and SD, are installed at QF and QD, respectively. These are further divided into two interleaved sub-families '1' and '2'. Only two SF and SD families are needed to correct the natural chromaticity of each ring. This includes the contributions from the arc and/or the contribution from the low-β insertions in collision. The present scheme can also correct the second order chromaticity and minimize the off-momentum beating induced by the inner triplet magnets in collision mode.

2.4.3 Lattice skew sextupoles, MSS

In each ring and each sector of the machine, four focusing sextupoles (2 SF1s and 2 SF2s situated mid arc) are rotated by 90° and are powered in series to generate a skew sextupole field for compensation of the chromatic coupling induced by the a_3 component of the main dipoles. This scheme guarantees extremely good compensation of the second order chromaticity induced by chromatic coupling, with a minimum impact on the third-order skew resonances and on the off-momentum β-beating.

2.4.4 Tune-shift or tuning quadrupoles, MQT

Two families of 8 tuning quadrupoles per ring and per sector, QTF and QTD, equip the short straight sections from Q14 to Q21 (left and right). Since the main quadrupole circuits are powered in series in Ring 1 and Ring 2, the phase advance per arc cell cannot be changed independently for

2008 JINST 3 S08001

the two beams. Therefore, independent tune adjustments for each beam can only be done by retuning the phase advances of the LHC insertions (essentially IR4) or by using the MQT corrector magnets. In principle, the latter are strong enough to achieve tune shifts of slightly more than one unit at 7 TeV. However, due to the large β-beating and dispersion mismatch induced, they will be limited to much smaller tune shifts in nominal operation, of the order of $\Delta Q \sim \pm 0.1$.

2.4.5 Arc skew quadrupole corrector magnets, MQS

In both rings, each sector of the machine is equipped with two pairs of skew quadrupole magnets MQS at Q23 and Q27 (left and right) which are just MQT type magnets rotated by 45°. The two pairs are either powered in series, in Sectors 1-2, 3-4, 5-6, 7-8 for Ring 1 and in Sectors 2-3, 4-5, 6-7, 8-1 for Ring 2, or split into two independent families in the other sectors. This layout allows compensation of the coupling coefficient due to the systematic $a2$ errors of the main dipoles for each sector, but implies that only four corrector circuits are available for correction of the random coupling errors. The betatron phase advances between the MQSs of the same family are such that the coupling compensation can be made without generating too large a vertical dispersion.

2.4.6 Landau damping or lattice octupoles, MO

Each short straight section not equipped with MQT or MQS type magnets contains a lattice octupole MO, making a total of 168 MO type magnets per ring, for the Landau damping of coherent oscillations caused by collective effects. These magnets will be powered in four families per sector, subdividing them into focusing and defocusing magnets, OF and OD, for Ring 1 and Ring 2.

2.4.7 Spool-piece corrector magnets

In addition to the lattice corrector magnets, each bore of the main dipoles will carry a small sextupole corrector magnet (MCS) at one end (Type B magnet), and every other dipole will be equipped with an octupole-decapole spool-piece (MCDO) at the opposite end (Type A magnet). The MCS magnets will be connected in series to form two families per sector, one for each ring. The same will apply for the octupole and decapole corrector magnets. The MCS spool-pieces are designed to compensate the b_3 field integral of the main dipoles in each sector of the machine, in order to correct its impact on the linear chromaticity up to top energy. On the other hand, the MCDO spool-piece corrector magnets mainly preserve the dynamic aperture of the LHC at injection.

2.5 High luminosity insertions (IR1 and IR5)

Interaction regions 1 and 5 house the high luminosity experiments of the LHC and are identical in terms of hardware and optics, except that the crossing-angle is in the vertical plane in Point 1 and in the horizontal plane in Point 5. The small β-function values at the IPs are generated between quadrupole triplets that leave ± 23 m free space about the IP. In this region, the two rings share the same vacuum chamber, the same low-beta triplet magnets, and the D1 separation dipole magnets. The remaining matching section (MS) and the dispersion suppressor (DS) consist of twin-bore

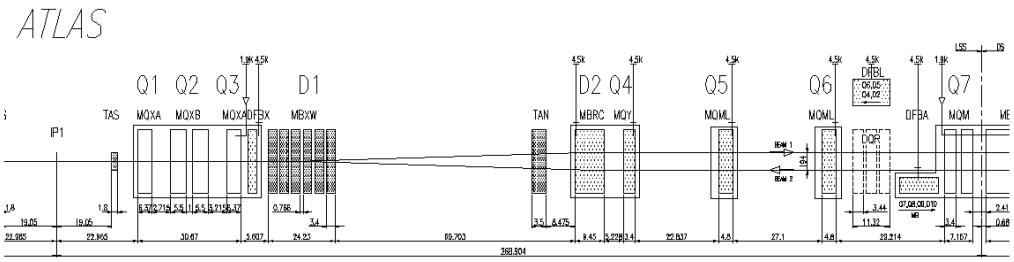

Figure 2.4: Schematic layout of the right side of IR1 (distances in m).

magnets with separate beam pipes for each ring. From the IP up to the DS insertion the layout comprises:

- A 31 m long superconducting low-β griplet assembly, operated at a temperature of 1.9 K and providing a nominal gradient of 205 T/m.
- A pair of separation / recombination dipoles separated by approximately 88 m.
- The D1 dipole located next to the triplet magnets, which has a single bore and consists of six 3.4 m long conventional warm magnet modules yielding a nominal field of 1.38 T.
- The following D2 dipole, which is a 9.45 m long, twin bore, superconducting dipole magnet, operating at a cryogenic temperature of 4.5 K with a nominal field of 3.8 T. The bore separation in the D2 magnet is 188 mm and is thus slightly smaller than the arc bore separation.
- Four matching quadrupole magnets. The first quadrupole following the separation dipole magnets, Q4, is a wide-aperture magnet operating at a cryogenic temperature of 4.5 K and yielding a nominal gradient of 160 T/m. The remaining three quadrupole magnets are normal-aperture quadrupole magnets, operating at a cryogenic temperature of 1.9 K with a nominal gradient of 200 T/m.

Figure 2.4 shows the schematic layout of IR1 on the right hand side. The triplet assembly features two different quadrupole designs: the outer two quadrupole magnets, made by KEK, require a peak current of 6450 A to reach the nominal gradient of 205 T/m, whereas the inner quadrupole block, consist of two quadrupole magnets made by FNAL, requires a peak current of 10630 A. The triplet quadrupoles are powered by two nested power converters: one 8 kA power converter powering all triplet quadrupole magnets in series and one 6 kA power converter supplying additional current only to the central two FNAL magnets. The Q1 quadrupole next to the IP features an additional 600 A trim power converter. Two absorbers protect the cold magnets from particles leaving the IP. The TAS absorber protects the triplet quadrupole magnets, and the TAN absorber, located in front of the D2 dipole magnet, protects the machine elements from neutral particles.

2.6 Medium luminosity insertion in IR2

The straight section of IR2 (see figures 2.5 and 2.6) houses the injection elements for Ring-1, as well as the ion beam experiment ALICE. During injection, the optics must obey the special con-

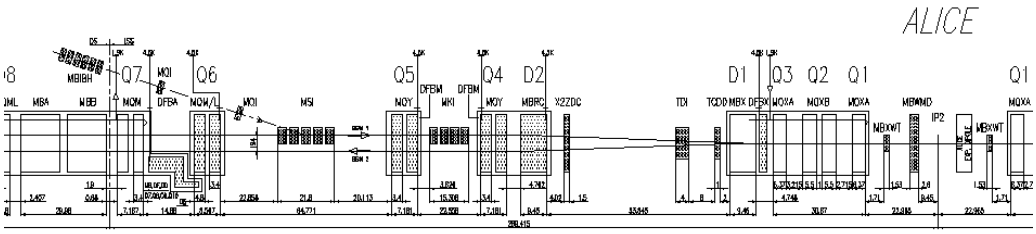

Figure 2.5: Schematic layout of the matching section on the left side of IR2 (distances in m).

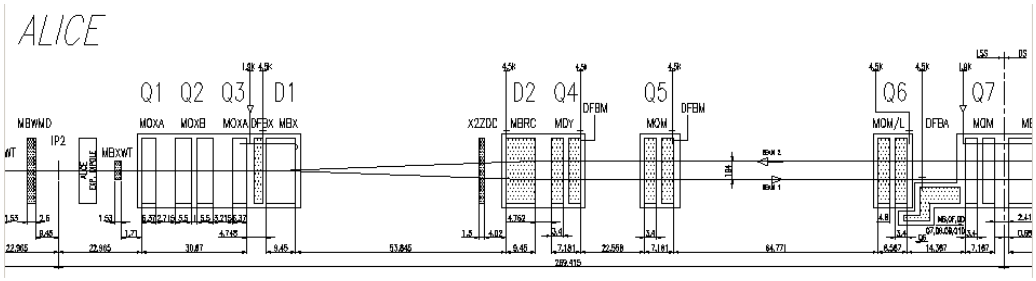

Figure 2.6: Schematic layout of the matching section on the right side of IR2 (distances in m).

straints imposed by the beam injection for Ring-1, and the geometrical acceptance in the interaction region must be large enough to accommodate both beams in the common part of the ring, with a beam separation of at least 10σ.

The triplet quadrupoles are powered in series and are followed by the separation / recombination dipoles D1 and D2, which guide the beams from the interaction region into two separated vacuum chambers. The quadrupoles Q4, Q5, Q6, Q7, Q8, Q9 and Q10 are individually powered magnets. The aperture of Q4 is increased to provide sufficient space for the crossing-angle orbit separation. The aperture of Q5 left of the IP is increased to provide sufficient aperture for the injected beam. The injection septum MSI is located between Q6 and Q5 on the left-side and kicks the injected beam in the horizontal plane towards the closed orbit of the circulating beam (positive deflection angle). The injection kicker MKI is located between Q5 and Q4 on the left-hand side of the IP and kicks the injected beam in the vertical plane towards the closed orbit of the circulating beam (negative deflection angle). In order to protect the cold elements in case of an injection failure, a large absorber (TDI) is placed 15 m upstream from the D1 separation / recombination dipole on the left side of the IP. The TDI absorber is complemented by an additional shielding element 3 m upstream of the D1 magnet and two additional collimators installed next to the Q6 quadrupole magnet. In order to obtain an optimum protection level in case of injection errors, the vertical phase advance between MKI and TDI must be 90°, and the vertical phase advance between the TDI and the two auxiliary collimators must be an integer multiple of 180°. The matching section extends from Q4 to Q7, and the DS extends from Q8 to Q11. In addition to the DS, the first two trim quadrupoles of the first arc cell (QT12 and QT13) are also used for matching.

2008 JINST 3 S08001

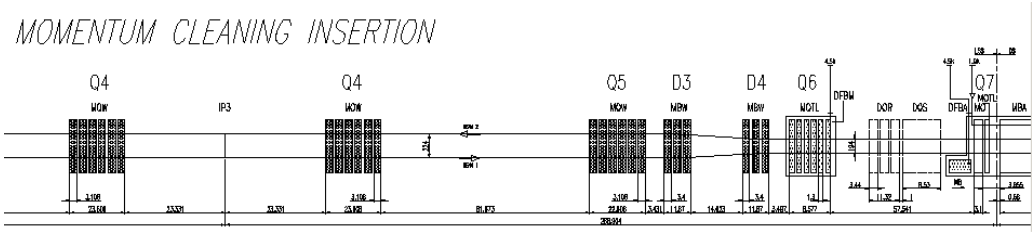

Figure 2.7: Schematic layout of the matching section on the right side of IR3 (distances in m).

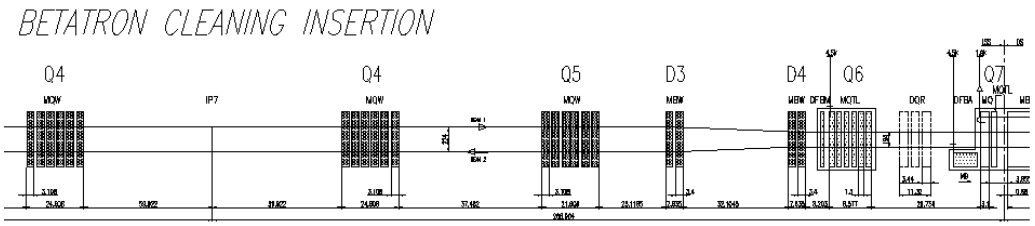

Figure 2.8: Schematic layout of the matching section on the right side of IR7 (distances in m).

2.7 Beam cleaning insertions in IR3 and IR7

The IR3 insertion houses the momentum cleaning systems of both beams, while IR7 houses the betatron cleaning systems of both beams. Particles with a large momentum offset are scattered by the primary collimator in IR3, and particles with a large betatron amplitudes are scattered by the primary collimator in IR7. In both cases, the scattered particles are absorbed by secondary collimators. Figures 2.7 and 2.8 show the right hand sides of IRs 3 and 7, respectively.

In IR7, the layout of the LSS between Q7L and Q7R is mirror symmetric with respect to the IP. This allows a symmetrical installation for the collimators of the two beams and minimizes the space conflicts in the insertion. Starting from Q7 left, the quadrupole Q6 (made of 6 superconducting MQTL modules) is followed by a dog-leg structure made of two sets of MBW warm single bore wide aperture dipole magnets (2 warm modules each). The dogleg dipole magnets are labelled D3 and D4 in the LHC sequence, with D3 being the dipole closer to the IP. The Primary Collimators are located between the D4 and D3 magnets, allowing neutral particles produced in the jaws to point out of the beam line, and most charged particles to be swept away. The inter-beam distance between the dogleg assemblies left and right from the IP is 224 mm, i.e., 30 mm larger than in the arc. This increased beam separation allows a substantially higher gradient in the Q4 and Q5 quadrupoles, which are made out of 6 warm MQW modules. The space between Q5 left and right from the IP is used to house the secondary collimators at appropriate phase advances with respect to the primary collimators.

In IR3, the most difficult constraint was to generate a large dispersion function in the straight section. Since the layout of the DS cannot be changed in IR3, this constraint means that the natural dispersion suppression generated in the DS is over-compensated. To fix this, Q6 and Q5 were moved towards each other by a substantial amount, thus shrinking the space granted to the dog-leg structure D4-D3. It was therefore necessary to add a third MBW element to D3 and D4 in IR3. Apart from this, IR3 and IR7 are identical.

2008 JINST 3 S08001

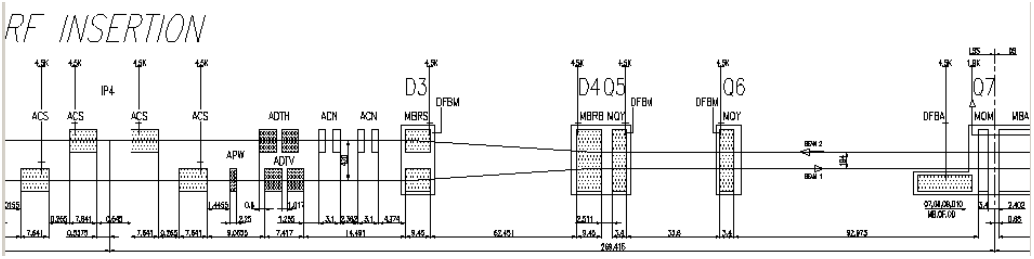

Figure 2.9: Schematic layout of the matching section on the right side of IR4 (distances in m).

2.8 RF insertion in IR4

IR4 (see figure 2.9) houses the RF and feed-back systems, as well as some of the LHC beam instrumentation. The RF equipment is installed in the old ALEPH (LEP) cavern, which provides a large space for the power supplies and klystrons. Because both RF systems are installed in this cavern, large drift spaces are necessary between the quadrupoles. This makes the insertion look similar to IR6. Furthermore, the two independent RF systems for Beam 1 and Beam 2 require a larger than nominal beam separation. The increased beam separation is provided by two pairs of dipole magnets. These dogleg dipole magnets are labelled D3 and D4 in the LHC sequence, with D3 being the dipole magnets closer to the IP. The inter-beam distance between the dogleg magnets is 420 mm, i.e., 226 mm larger than in the arcs. In contrast to IR3 and IR7, the dogleg magnets in IR4 are superconducting.

2.9 Beam abort insertion in IR6

IR6 (see figure 2.10) houses the beam abort systems for Beam 1 and Beam 2. Beam abort from the LHC is done by kicking the circulating beam horizontally into an iron septum magnet, which deflects the beam in the vertical direction away from the machine components to absorbers in a separate tunnel. Each ring has its own system, and both are installed in IR6. In order to minimize the length of the kicker and of the septum, large drift spaces are provided. Matching the β-functions between the ends of the left and right DS requires only four independently-powered quadrupoles. In each of the dispersion suppressors, up to six quadrupoles can be used for matching. The total of sixteen quadrupoles is more than sufficient to match the β-functions and the dispersion, and to adjust the phases. There are, however, other constraints to be taken into account concerning apertures inside the insertion.

Special detection devices protect the extraction septum and the LHC machine against losses during the abort process. The TCDS absorber is located in front of the extraction septum and the TCDQ in front of the Q4 quadrupole magnet downstream of the septum magnet.

2.10 Medium luminosity insertion in IR8

IR8 houses the LHCb experiment and the injection elements for Beam 2 (see figures 2.11 and 2.12). The small β-function values at the IP are generated with the help of a triplet quadrupole assembly

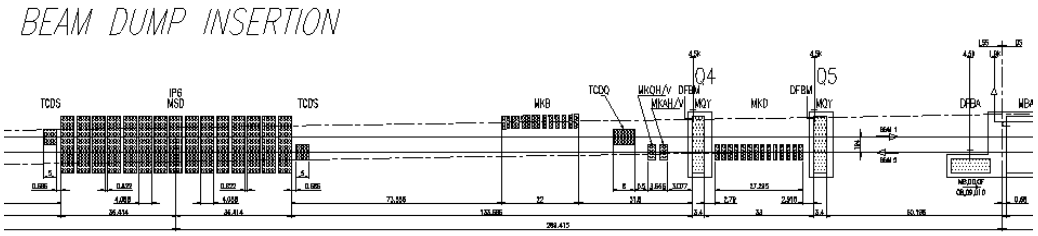

Figure 2.10: Schematic layout of the matching section on the right side of IR6 (distances in m).

that leaves ± 23 m of free space around the IP. In this region, the two rings share the same vacuum chamber, the same low-beta triplet magnets, and the D1 separation dipole magnet. The remaining matching section (MS) and the DS consist of twin-bore magnets with separate beam pipes for each ring. From the IP up to the DS insertion the layout comprises:

- Three warm dipole magnets to compensate the deflection generated by the LHCb spectrometer magnet.
- A 31 m long superconducting low-β triplet assembly operated at 1.9 K and providing a nominal gradient of 205 T/m.
- A pair of separation / recombination dipole magnets separated by approximately 54 m. The D1 dipole located next to the triplet magnets is a 9.45 m long single-bore superconducting magnet. The following D2 dipole is a 9.45 m long double bore superconducting dipole magnet. Both magnets are operated at 4.5 K. The bore separation in the D2 magnet is 188 mm and is thus slightly smaller than the arc bore separation.
- Four matching quadrupole magnets. The first quadrupole following the separation dipole magnets, Q4, is a wide aperture magnet operating at 4.5 K and yielding a nominal gradient of 160 T/m. The remaining three matching section quadrupole magnets are normal aperture quadrupole magnets operating at 1.9 K with a nominal gradient of 200 T/m.
- The injection elements for Beam 2 on the right hand side of IP8. The 21.8 m long injection septum consists of 5 modules and is located between the Q6 and Q5 quadrupole magnets on the right-hand side of the IP. The 15 m long injection kicker consists of 4 modules and is located between the Q5 and Q4 quadrupole magnets on the right-hand side of the IP. In order to protect the cold elements in case of injection failure, a large absorber (TDI) is placed 15 m in front of the D1 separation / recombination dipole magnet, right from the interaction point. The TDI is complemented by an additional shielding element (TCDD) between the TDI and D1 magnet (placed 3 m in front of D1) and by two additional collimators, placed at the transition of the matching section, left from the interaction point, to the next DS section.

In order to provide sufficient space for the spectrometer magnet of the LHCb experiment, the beam collision point is shifted by 15 half RF wavelengths (3.5 times the nominal bunch spacing ≈ 11.25 m) towards IP7. This shift of the collision point has to be compensated before the beam returns to the dispersion suppressor sections and requires a non-symmetric magnet layout in the matching section.

2008 JINST 3 S08001

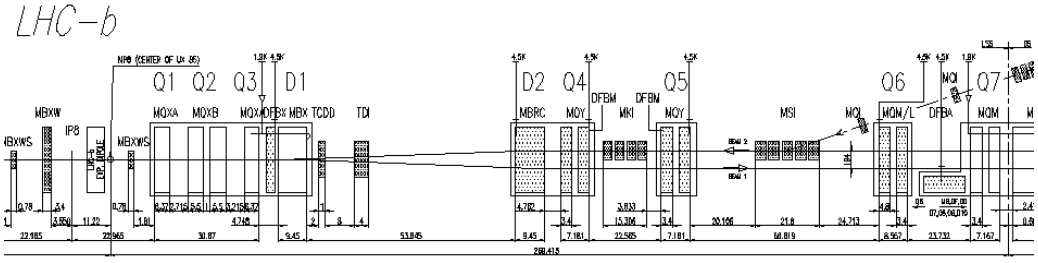

Figure 2.11: Schematic layout of the matching section on the right side of IR8 (distances in m).

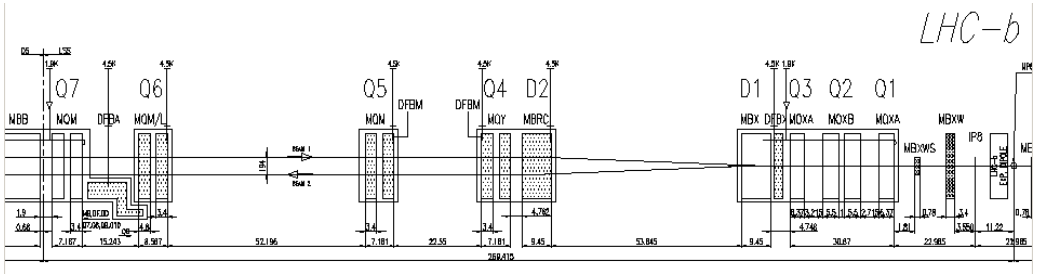

Figure 2.12: Schematic layout of the matching section on the left side of IR8 (distances in m).